Biomedicine & Pharmacotherapy 180 (2024) 117532

Contents lists available at ScienceDirect

Biomedicine & Pharmacotherapy

journal homepage: www.elsevier.com/locate/biopha

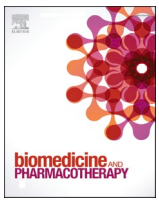

Protective effects of lemon nanovesicles: evidence of the Nrf2/HO-1 pathway contribution from *in vitro* hepatocytes and *in vivo* high-fat diet-fed rats

Roberta Gasparro [a,1], Giuditta Gambino [b,1], Giulia Duca [a], Danila Di Majo [b], Valentina Di Liberto [b], Vincenza Tinnirello [a], Giulia Urone [b], Nicolò Ricciardi [b], Monica Frinchi [b], Nima Rabienezhad Ganji [a], Giuseppe Vergilio [c], Francesco Paolo Zummo [c], Francesca Rappa [c,d], Simona Fontana [a], Alice Conigliaro [a,e,f], Pierangelo Sardo [b], Giuseppe Ferraro [b], Riccardo Alessandro [a,f,g,2], Stefania Raimondo [a,f,*,2]

[a] *Department of Biomedicine, Neurosciences and Advanced Diagnostics (Bi.N.D), University of Palermo, Section of Biology and Genetics, Palermo 90133, Italy*
[b] *Department of Biomedicine, Neurosciences and Advanced Diagnostics (Bi.N.D), University of Palermo, Section of Human Physiology, Palermo 90134, Italy*
[c] *Department of Biomedicine, Neurosciences and Advanced Diagnostics (BIND), Institute of Human Anatomy and Histology, University of Palermo, Palermo 90127, Italy*
[d] *The Institute of Translational Pharmacology, National Research Council of Italy (CNR), 90146 Palermo, Italy*
[e] *ATeN (Advanced Technologies Network) Center, Viale Delle Scienze, University of Palermo, 90128, Palermo, Italy*
[f] *Navhetec s.r.l., Spinoff of the University of Palermo, Palermo, Italy*
[g] *Institute for Biomedical Research and Innovation (IRIB), National Research Council (CNR), Palermo 90146, Italy*

ARTICLE INFO

Keywords:
Lemon-derived nanovesicles
Oxidative stress
Liver
High-fat diet fed rats
Metabolic syndrome

ABSTRACT

The cross-talk between plant-derived nanovesicles (PDNVs) and mammalian cells has been explored by several investigations, underlining the capability of these natural nanovesicles to regulate several molecular pathways. Additionally, PDNVs possess biological proprieties that make them applicable against pathological conditions, such as hepatic diseases. In this study we explored the antioxidant properties of lemon-derived nanovesicles, isolated at laboratory (LNVs) and industrial scale (iLNVs) in human healthy hepatocytes (THLE-2) and in metabolic syndrome induced by a high-fat diet (HFD) in the rat. Our findings demonstrate that in THLE-2 cells, LNVs and iLNVs decrease ROS production and upregulate the expression of antioxidant mediators, Nrf2 and HO-1. Furthermore, the *in vivo* assessment reveals that the oral administration of iLNVs improves glucose tolerance and lipid dysmetabolism, ameliorates biometric parameters and systemic redox homeostasis, and upregulates Nrf2/HO-1 signaling in HFD rat liver. Consequently, we believe LNVs/iLNVs might be a promising approach for managing hepatic and dysmetabolic disorders.

1. Introduction

The imbalance between reactive oxygen species (ROS) and antioxidant systems is known as oxidative stress. Generally, oxidants can act as crucial regulators of several physiological and non-physiological processes such as cell proliferation, inflammation, autophagy, and response to stress. ROS are formed during oxidative metabolic activities [1] and in reaction to exogenous signals, including pathogens [2,3], or endogenous signals like cytokines [4]. Uncontrolled production of ROS induces cell toxicity and could lead to the development of tumors and chronic diseases due to their capability to be harmful to DNA, proteins, and lipids. The liver is the main organ in charge of controlling metabolism and detoxification and hence is particularly subjected to oxidative stress damage. Both extrinsic (alcohol, drugs, toxins, viruses, and smoking) and intrinsic (obesity and insulin resistance) sources [5] can cause liver chronic inflammation and elicit immune cell activation and oxidative

* Corresponding author at: Department of Biomedicine, Neurosciences and Advanced Diagnostics (Bi.N.D), University of Palermo, Section of Biology and Genetics, Palermo 90133, Italy.
E-mail address: stefania.raimondo@unipa.it (S. Raimondo).
[1] Co-First authors
[2] Co-last authors

https://doi.org/10.1016/j.biopha.2024.117532
Received 29 July 2024; Received in revised form 26 September 2024; Accepted 4 October 2024
Available online 8 October 2024

stress. Excessive ROS within hepatocytes can induce hepatic structural and functional abnormalities that lead to a variety of disorders, such as Non-Alcoholic Fatty Liver Disease (NAFLD), Alcoholic Fatty Liver Disease (AFLD), fibrosis, and Hepatocellular Carcinoma (HCC) [6]. The nuclear E2-related factor 2 (Nrf2) pathway is one of the most important adaptive stress responses involved in the prevention and reduction of hepatic damage [7]. Nrf2 is a positive regulator of the human Antioxidant Response Element (ARE), confined in the cytoplasm by the suppressor protein Keap1 [8]. Translocation into the nucleus triggers the expression of multiple antioxidant enzymes, including heme oxygenase 1 (HO-1) which controls oxidative stress, inflammation, and inhibits apoptosis by removing toxic heme [9,10].

Among the *in vivo* models widely used and selected to study liver disease, literature has agreed on the importance of high-fat diets (HFD) inducing a reliable model of Metabolic Syndrome (MetS) [11,12]. Undoubtedly, the ability of natural compounds to positively influence HFD-induced metabolic syndrome is well-known [13–15] and could provide solid bases of prediction for translational studies [16].

In detail, a specific dietary regimen with HFD is able to replicate the full clinical spectrum of increased body weight, glucose intolerance, dyslipidemia, and hepatic dysfunction. The alterations in metabolic state are linked to profound modifications of redox homeostasis that trigger widespread tissue dysfunction, especially in the liver [17,18]. Our recent research demonstrated that specific systemic biomarkers of redox homeostasis are strong predictors of metabolic dysfunction development, emphasizing the significant role of oxidative alterations in MetS [17]. Remarkably, the disrupted balance between oxidative stress indicators and antioxidant defenses has been identified in HFD rat models, affecting systemic homeostasis and tissues, including the brain and the liver, and interfering with crucial signaling pathways such as Nrf2. [19,20]. Among other biomarkers, the levels of plasmatic products of lipid peroxidation are increased after 10 weeks of HFD in rats [21,22] and their liver exhibits hepatic lipid peroxidation and dysfunction [23]. This hepatic oxidative damage can contribute to the development of NAFLD by exacerbating the deposition of extracellular matrix and hepatic fibrosis [24].

Currently, the substantial worldwide impact of chronic liver disease has spurred intensive research into alternative treatment options. Additionally, the scarcity of available organs for transplantation, which represents the definitive cure for end-stage liver disease, has underscored the urgent demand for novel therapies [25]. One of the interactions that is attracting the interest of biomedical scientists due to its therapeutic potential is cross-kingdom communication, i.e. the ability of organisms from one kingdom to regulate the biological and molecular mechanisms of organisms of another kingdom. Today, it is known that extracellular vesicles (EVs) act as a shared mode of communication among living organisms from different kingdoms. In particular, during intercellular communication, various cell types, such as those in animals, plants, and microorganisms, release EVs that are composed of a lipid bilayer. Recently, there has been an increasing interest in exploring the potential cross-kingdom communication roles of these vesicles, particularly in comprehending interactions between vesicles derived from plants and mammalian cells. Extracellular vesicles derived from plants can be extracted from different fruits and vegetables, such as lemon [26,27], blueberry [28], tomato [29], grapefruit [30], garlic [31], and more. These nanovesicles contain lipids [32], proteins [26], nucleic acids [33], and metabolites in their cargo [34]. Recently, a novel breakthrough has emerged in the form of Decoctosomes and Bencaosomes, nanoparticles derived from boiled Chinese herbal medicines. These nanoparticles contain active ingredients such as small molecules, peptides, and small RNAs (sRNAs). Enhanced versions of Decoctosomes, known as Bencaosomes, have demonstrated effectiveness in disease models, underlying their potential in nucleic acid therapy [35]. Furthermore, numerous studies have underscored the biological properties of PDEVs, including their demonstrated anti-cancer [26], anti-inflammatory [36], and antioxidant activities [37]. Zhao et al. found that the administration of blueberry-derived exosomes-like nanoparticles modulated the expression of antioxidant genes through Nrf2 activation, enhanced hepatic function, prevented the formation of vacuoles, and mitigated the buildup of lipid droplets in the livers of mice subjected to a high-fat diet [28]. In a recent study, garlic-derived exosomes showed their anti-inflammatory activity in THP-1 macrophages and decreased the accumulation of lipid droplets in high-fat diet (HFD)-feeding mice liver [31]. Exosome-like nanovesicles derived from garlic also possess the ability to hinder the migration and infiltration of macrophages into the liver to prevent hepatocyte apoptosis and inflammasome activation [38]. Our recent studies revealed that nanovesicles extracted from *Citrus* limon juice (LNVs) produce anti-inflammatory effects in murine and human immune cells by inhibiting the NF-κB/ERK1–2 signaling pathways. [39] and possess antioxidant activity in human dermal fibroblasts and zebrafish thanks to their capability to induce the activation of the AhR/Nrf2 signaling pathway [27].

In this study, we investigate for the first time the hepatoprotective effect of LNVs exploiting *in vitro* and *in vivo* models. To achieve this, we studied the antioxidant properties of LNVs in human healthy hepatocytes (THLE-2) and their hepatoprotective effects in MetS rats fed with HFD. The integration of data from both *in vitro* and *in vivo* experiments is crucial to carry out a comprehensive understanding of the mechanisms and potential therapeutic benefits of lemon-derived nanovesicles in liver protection.

2. Materials and methods

2.1. LNVs and iLNVs isolation

LNVs were obtained from lemons coming from a private farmer as previously described [27,39]. The juice was produced by manual squeezing and processed using the following differential centrifugations protocol: two centrifuges at 3000 g for 15 minutes, two centrifuges at 10,000 g for 30 minutes, a filtration step with a 0.8 μm pores filter, a centrifuge at 16,500 g for 1 h, followed by another filtration with 0.45 μm filters, and a final centrifuge at 16,500 g for 3 h were performed. At the end of the process, the supernatant was collected and ultracentrifuged at 100,000 g for 1.45 h. The pellet obtained was resuspended in PBS. Industrial-derived Nanovesicles (iLNVs) were produced using a patented process (IT patent n° 102019000005090, "Process for the production of vesicles from citrus juice") and were characterized as shown in our previous study [40]. Briefly, the lemon juice, obtained by Agrumaria Corleone s.p.a. (Palermo, Italy), was ultrafiltered with pore size 50,000 Dalton. The retentate was then microfiltrated at 0.45 μm, obtaining a permeate containing the vesicles. Quantification of LNVs and iLNVs was performed by the Bradford protein assay (Pierce, Rockford, IL, USA) with Coomassie Brilliant Blue and the reading was finally performed using a biophotometer.

2.2. Cell line and culture conditions

THLE-2 cell line (T-antigen immortalized Human Liver Epithelial cell – ATCC CRL-2706™, LGC Standards, Manassas, VA, USA) was used as an *in vitro* model of healthy human hepatocytes. Cells were cultured on 0.03 mg/mL bovine collagen type I coating (Advanced Biomatrix, San Diego region, CA, USA) and 0.01 mg/mL bovine serum albumin (Sigma-Aldrich, St Louis, MO, USA) and kept for 24 h in an incubator at 37°C at 5 % CO_2. THLE-2 cell line was cultured in RPMI 1640 medium (Euroclone, UK), with the addition of 10 % fetal bovine serum (FBS, Euroclone, UK), 1 % penicillin (100 U/mL) and streptomycin (100 μg/mL), 0.3 mL of human recombinant Epidermal Growth Factor (EGF) (10 μg/mL), and 0.4 mL of phosphoethanolamine (PEA) (100 μg/mL.

2.3. Vesicles internalization assay

The internalization of LNVs and iLNVs in THLE-2 was evaluated by confocal microscopy. LNVs and iLNVs were incubated at room temperature with the lipophilic dye PKH26 (10 μM) for 20 minutes. Once the incubation time was over, the labeled vesicles were centrifuged at 14,000 rpm for 10 minutes to eliminate the excess of unbound dye. The pellet obtained was subjected to 4 washes in PBS and finally resuspended in RPMI medium 1640. THLE-2 cells were seeded at 3×10^4 cells per well in 8-well chamber (Thermo Scientific Nunc, Waltham, MA, USA). After 24 h, cells were treated for 2 h and 6 h with the labeled LNVs (10 μg/mL and 25 μg/mL) or iLNVs (2.5 μg/mL). After the treatment, cells were fixed with PFA 4 % and membranes were temporarily permeabilized with 0.1 % Triton. Cell staining was performed by incubating for 30 minutes with Hoechst (Invitrogen Biosystems, Thermo Fisher Scientific, Waltham, MA, USA) prepared 1:1000 in PBS and Actin Green (Invitrogen Biosystems, Thermo Fisher Scientific, Waltham, MA, USA). The internalization of LNVs and iLNVs in target cells was analyzed through confocal microscopy (Nikon A1).

2.4. Cell viability assay

The 3-(4,5-Dimethylthiazol-2-yl)-2,5-Diphenyltetrazolium Bromide (MTT) colorimetric assay was used as an indicator of cell viability. The MTT assay was performed to establish doses of nanovesicles that were not toxic to THLE-2; cells were seeded in triplicate, in a 96-well plate (1×10^4 cells per well) and after 24 h were subjected to 24 h treatment with LNVs (10 μg/mL, 25 μg/mL) or with iLNVs (2.5 μg/mL). At the end of the treatment, the MTT solution (5 mg/mL stock) was added to each well in a 1:10 ratio. After 3 hours of incubation, the reaction was stopped with the addition of isopropanol HCl (1 +1/2 of the volume in each well). Absorbance was determined using an ELISA reader set to 540 nm (Microplate Reader, BioTek, Winooski, VT, USA).

2.5. ROS quantification assay

The 2′,7′-dichlorodihydrofluorescein diacetate (H2DCFDA) probe was used to perform ROS quantification assay in THLE-2 pre-treated with LNVs (10 μg/mL and 25 μg/mL) or with iLNVs (2.5 μg/mL) and exposed to menadione (5 μM and 10 μM). The probe, excited at a wavelength of 485 nm, emits a signal at 535 nm (blue reading) detected by fluorescence spectroscopy. THLE-2 were seeded in triplicate, 1×10^4 per well, in a 96-well plate (Nunclon Delta Surface 96-well plate by Thermo Fisher Scientific, Waltham, MA, USA), and after 24 h cells were pre-treated with LNVs or iLNVs. At the end of 24 hours, the medium containing the vesicles was removed and, in a medium FBS-free, the probe (10 μM) and the menadione (5 or 10 μM) were added at the same time. Using the Glomax Multi Detection Plate Reader (Promega, Madison, WI, USA), a reading of the fluorescence emitted was carried out to quantify the level of intracellular ROS.

2.6. RNA isolation, cDNA synthesis and Real-time PCR

8×10^4 cells were seeded in a 12-well plate. Cells were pre-treated for 24 h with vesicles (10 μg/mL and 25 μg/mL) or with iLNVs (2.5 μg/mL) and then treated for 30 minutes with menadione (5 μM), added without medium removal. HFD-fed rats were administered with iLNVs as reported in the "2.9 *In Vivo* Model" section. Total RNA was purified from cells using Nucleospin miRNA Kit (Macherey-Nagel, Düren, Germany) and from animal biopsies with NucleoSpin RNA Set for NucleoZOL (Macherey-Nagel, Düren, Germany). The total RNA was quantified with Nanodrop spectrophotometer (NanoDrop Technologies, Wilmington, NC, USA) and Retrotranscription from RNA to cDNA was executed using the High-Capacity cDNA Reverse Transcription kit (Applied Biosystems, Foster City, CA, USA). Real-time PCR was performed with SYBR Green mix (Applied Biosystems, Foster City, CA, USA). Modulations in target genes were determined, relative to actin, using the ΔΔCt method.

2.7. Western blot

THLE-2 were seeded 3×10^5 per flask (T25), pre-treated for 24 h with 10 μg/mL and 25 μg/mL of LNVs or with 2.5 μg/mL of iLNVs, and treated with 5 μM menadione for 30 minutes. Once the treatment time was over, the cells were collected and resuspended in PBS. HFD-fed rats were administered with iLNVs as reported in the "2.9 *In Vivo* Model" section. The liver tissue was collected after the animals had been sacrificed and cut into smaller pieces. THLE-2 cells and hepatic biopsies were resuspended in a lysis buffer (consisting of 50 mM Tris-HCl pH 7.6, 300 mM NaCl, 0.5 % TritonX-100, 1X PMSF, 1X leupeptin, 1X aprotinin, phosphatase inhibitors 1X (Phosphatase inhibitor cocktail 10X) and H_2O milliQ). Quantitation was performed using Coomassie Brilliant Blue and a biophotometer. The samples for the WB were then prepared: adding the H_2O, the sample buffer (4X) and the reducing agent (10X) to the proteins and denaturing them for 10 minutes at 70°C. Samples were loaded onto an SDS-page BoltTM 4–12 % Bis-Tris Plus gel (Invitrogen, Waltham, MA, USA) and, in the presence of a running buffer consisting of MES and H_2O. After the electrophoretic run at 165 V, the transfer of the proteins from the gel to a nitrocellulose membrane (Amersham, Healthcare Life Sciences, Little Chalfont, Buckinghamshire, UK) inserted into transfer buffer (20 % methanol, H_2O, 10X trisglycine) was completed at 50 V. The membrane was incubated at 4°C for 1.30 h with 1 % BSA to block the non-specific antibody binding sites. The primary antibody (prepared in BSA 1 %) was incubated overnight at 4°C. The following day the secondary antibody was added (1:1000 in BSA 1 %) at 4°C for 1 h. The primary antibodies used were anti-Nrf2 (Novus Biologicals, Centennial, CO, USA), anti-HO-1 (Bioworld Technology, Antibodies, St. Louis Park, MN, USA), anti-β-actin (Santa Cruz Biotechnology, Santa Cruz, CA, USA). The Amersham ECL Western Blotting Detection Reagent solution (Detection Reagent 1 and 2 in a 1:1 ratio) (GE Healthcare Life Sciences, Little Chalfont, Buckinghamshire, UK) allowed the detection of the chemiluminescence signal and the highlighting of the protein band using the "ChemiDocTMMP" (Bio-rad, Hercules, CA, USA). "Image Lab" software was utilized for the densitometric analysis of the bands.

2.8. Immunofluorescence assay

To evaluate the nuclear Nrf2 expression after the pre-treatment with LNVs/iLNVs and the following treatment with menadione, immunofluorescence protocol was performed, and the signal was detected by confocal microscopy. 25×10^3 cells per well were plated on an 8-well chamber (Thermo Scientific Nunc, Waltham, MA, USA) and these were pre-treated for 24 hours with LNVs (10 μg/mL and 25 μg/mL) or with iLNVs (2.5 μg/mL). The day after, cells were treated for 30 minutes with menadione (5 μM). Once the treatment time with menadione was over, THLE-2 cells were fixed with PFA 4 % for 10 minutes. After the permeabilization of membranes with Triton 0.1 %, the incubation for 1 h with the anti-Nrf2 primary antibody (Novus Biologicals, Centennial, CO, USA) diluted 1:200 in 1 % BSA and then the incubation for 1 h with the secondary antibody (Goat anti-Rabbit IgG H+L Secondary Antibody, DyLight™ 594, Invitrogen Biosystems, Thermo Fisher Scientific, Waltham, MA, USA) prepared 1:500 in 1 % BSA was performed. Nuclei and cytoskeleton were respectively labeled for 30 minutes with Hoechst (Invitrogen Biosystems, Thermo Fisher Scientific, Waltham, MA, USA) prepared 1:1000 in PBS and Actin Green (Invitrogen Biosystems, Thermo Fisher Scientific, Waltham, MA, USA). The Nikon A1 confocal microscope (Amsterdam, Netherlands) was used to observe the fluorescence. The amount of nuclear and total Nrf2 was quantified using the NIS-Elements Software. The nuclear Nrf2 was calculated by measuring the media of fluorescence of the Region of interest (ROI) in the nuclei for each field analyzed (n=7–9). The total Nrf2 was calculated by measuring the media of total fluorescence associated with the ROI

Table 1
Oligonucleotides used in qRT-PCR.

Human	Forward Sequence (5to 3)	Reverse Sequence (5to 3)
ACTIN	TCCCTTGCCATCCTAAAAAGCCACCC	CTGGGCCATTCTTCCTTAGAGAGAAG
NRF2	CACATCCAGTCAGAAACCAGTGG	GGAATGTCTGCGCCAAAAGCTG
HO−1	CCAGGCAGAGAATGCTGAGTTC	AAGACTGGGCTCTCCTTGTTGC
Rat	Forward Sequence (5to 3)	Reverse Sequence (5to 3)
ACTIN	AAGGCCAACCGTGAAAAGAT	TGGTACGACCAGAGGCATAC
NRF2	CACATCCAGACAGACACCAGT	CTACAAATGGGAATGTCTCTGC
HO−1	ACAGGGTGACAGAAGAGGCTAA	CTGTGAGGGACTCTGGTCTTTG

divided by the number of nuclei of every single field (n=7–9).

2.9. In Vivo model

2.9.1. Animals and diet composition

Male Wistar rats (9-week-old, n = 10) were obtained from Envigo S.r.l (Indianapolis, Indiana) and housed in pairs with a 12-hour light/dark cycle from 8:00–20:00 h with stable conditions of temperature (22–24 ∘C) and humidity (50 ± 10 %). Once in the animal facility, rats were maintained in a 7-day acclimation period, initially receiving a standard chow diet (i.e.3.94 kcal/g). After this period, they were weighed to exclude eventual initial differences and included into two uniform groups that were both fed with a high-fat diet (HFD) provided by Mucedola (Milan, Italy), whose code is "PF4215-PELLET". This diet allows to derive 60 % of energy from fats since it is a hypercaloric pelletized diet (5.5 Kcal/g) with 34 % fat, 23 % protein, 38 % carbohydrates, and 5 % fiber, that was provided for 10 weeks to induce MetS based on established criteria from previous literature [13];[18]. Throughout the experiment, all rats had unrestricted access to food and water. Animal experimentantion adhered to the ARRIVE guidelines and the European Directive (2010/63/EU). The University of Palermo's animal welfare committee approved the experimental protocols, and the Ministry of Health (Rome, Italy) granted authorization (Authorization Number n° 386/2024-PR).

2.9.2. Experimental design and nutritional supplementation

The experimental *in vivo* study is segmented into three distinct phases: T0 (initiation), T1 (Metabolic Syndrome induction), and T2 (experiment conclusion):

- Initial Group Allocation (T0): following the acclimatization phase (7 days), animals were fed with HFD for 10 weeks until the induction of Metabolic Syndrome.
- Metabolic Syndrome Induction and Group Stratification (T1): Verification of Metabolic Syndrome induction was performed at T1 after 10 weeks of HFD, employing established protocols.[13];[18] Animals were subsequently stratified into two groups relatively to the nutritional treatment received (iLNVs or vehicle) from T1 until T2, reached four weeks after T1. The HFD-iLNVs group (n=6) received daily iLNVs supplementation until T2, while the second group (HFD, n=4) representing the Metabolic Syndrome control was fed with the HFD and received daily gavage of vehicle (water) until T2 to make sure that they were under identical stress conditions as the HFD-iLNVs group.
- Experiment Conclusion (T2): This timepoint represents the end of the experimental study, occurring 14 weeks after the beginning (T0). Animals were sacrificed at T2 following authorized procedures to perform subsequent *ex-vivo* analyses.

Fig. 1 illustrates the experimental plan of the *in vivo* study.

2.9.2.1. Dietary supplementation with iLNVs. Dietary supplementation with iLNVs involved oral gavage administration with a daily volume of 1 mL, corresponding to 1.2 mg/Kg for 4 weeks (T1-T2).

2.9.3. Evaluation of biometric, biochemical, and oxidative homeostasis parameters

The evaluation of *in vivo* parameters was performed at T2 to explore the *in vivo* effects of iLNVs on MetS-induced alterations via biometric,

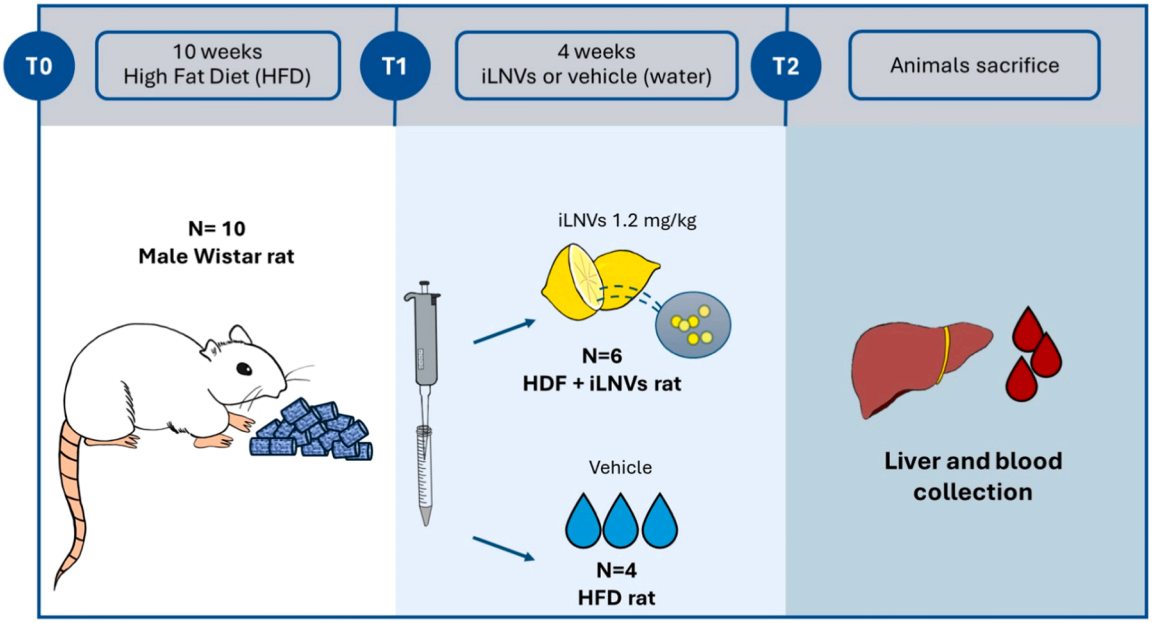

Fig. 1. : Representation illustrating the metabolic syndrome development in rats and the proposed treatment design.

biochemical, and oxidative homeostasis assays, after euthanasia in adherence to authorized protocols. Plasma samples were gathered for subsequent analyses, encompassing assessments of glucose and lipid homeostasis, oxidative stress parameters, and plasma antioxidant status. Additionally, hepatic samples were collected for *ex-vivo* evaluations.

2.9.3.1. Body weight gain evaluation. The evaluation of body weight of all the animals was performed throughout the experiment to evidence eventual differences between groups. In particular, we evaluated the final weight reached by all animals and we calculated the body weight gain, i.e. the Delta Body Weight (ΔBW), considering the final rat weight with respect to the initial weight recorded at T0.

2.9.3.2. Evaluation of glucose and lipid homeostasis. To assess the impact of nutritional treatments on glucose homeostasis in Metabolic Syndrome, we performed a Glucose Tolerance Test (GTT) at T2 following previously established methods [13] to. In summary, after fasting overnight, we collected a blood sample from the tail vein to obtain a baseline measurement using a Glucometer (Glucotest, Pic). Subsequently, a 20 % glucose solution was injected intraperitoneally (2 g/kg body weight), and blood glucose levels were recorded at 30-, 60- and 120 minutes post-injection. The area under the curve (AUC) was then derived for the experimental groups based on blood glucose levels (mg/dL) over time. For lipid homeostasis analysis, blood samples were collected from each animal at T2 after sacrifice through cardiac puncture. Detailed methods, as outlined in our previous study [13] were used to assess the effect of iLNVs supplementation. Plasma concentrations of triglycerides (TG), total cholesterol (TC), low-density lipoprotein cholesterol (LDL), and high-density lipoprotein cholesterol (HDL) were measured using commercial kits with the Free Carpe Diem device (FREE® Carpe Diem; Diacron International, Grosseto, Italy). Results are presented as mg/dL.

2.9.3.3. Oxidative stress parameters and plasma antioxidant status. The evaluation of plasma redox balance at T2 was conducted using Diacron kits, as described in our earlier publications [13]. Prooxidant status was determined through the dROMs (Reactive Oxygen Metabolites) and LP-CHOLOX tests. Levels of hydroperoxides, lipoperoxides, and oxidized cholesterol were measured utilizing the Free Carpe Diem device (FREE® Carpe Diem; Diacron International, Grosseto, Italy). Data from dROMs tests are presented in Carratelli units (UCARR), with the normal range being 250–300 U. CARR, where 1 U. CARR is equivalent to 0.08 mg/dL of H_2O_2.[41] The LP-CHOLOX test results, which indicate lipoperoxides and oxidized cholesterol levels, are expressed in mEq/L.

Regarding plasma antioxidant status, the SHp test assessed thiol groups' reducing properties, gauging the potential of iLNVs extracts to counteract thiol group oxidation and favor reduced forms. Furthermore, we investigated the levels of anti-ROMs, which is a colorimetric method based on the ability of plasma antioxidants to reduce ferric iron to ferrous iron which reacting with a specific chemical compound gives rise to reddish-purple solution [42]. The Anti-ROMs Test develops the reaction in two stages: in the first, it evaluates rapid exogenous antioxidants called "fast" such as Vitamin C and vitamin E ("exogenous anti-ROMs") and after it reveals "slow" antioxidants such as uric acid, thiol group, bilirubin, and polyphenols ("endogenous anti-ROMs"). The analysis was performed on previously heparinized plasma samples using a photometer (FREE® Carpe Diem) and measurements were conducted by commercial kits (Diacron International, Grosseto, Italy). For the interpretation of the results, reference values were used according to data reported in the literature [42], which predict optimal values for exogenous antioxidant defenses over 200 μEq/L and for endogenous antioxidant defenses values over 1000 μEq/L. Otherwise, values of exogenous antioxidants below 100 μEq/L and endogenous antioxidants below 500 μEq/L are considered high deficiency.

2.10. Immunohistochemistry

The immunohistochemical reactions were carried out on 5 μm thick hepatic tissue sections, obtained from paraffin blocks, as previously described in detail [40]. The primary antibody used was anti-Nfr2 (rabbit polyclonal antibody, NOVUS BIO-Techne Abingdon, United Kingdom, NBP1–32822 dilution 1:200). An optical microscope (Microscope Axioscope 5/7 KMAT, Carl Zeiss, Milan, Italy) with a digital camera (Microscopy Camera Axiocam 208 color, Carl Zeiss, Milan, Italy) was used to observe the slides. Immunopositivity was evaluated at high-power-field (HPF, magnification 400x), conducted over 10 HPFs, with the results expressed as a percentage.

2.11. Statistical analysis

Statistical analysis was performed using GraphPad Prism software (Version 10.1.0 (316), GraphPad Software, Inc., La Jolla, CA, USA). The Shapiro–Wilk test was used to evaluate the normal distribution of the data. For normally distributed datasets, an unpaired two-tailed Student's t-test was employed to determine statistical significance between groups. When data did not pass the normality test, the non-parametric Mann-Whitney test was applied for comparisons. Differences were considered significant when $p < 0.05$. The results are presented as the mean ± standard deviation (SD).

3. Results

3.1. Internalization of LNVs and iLNVs in THLE-2 cells

Lemon nanovesicles were in-depth characterized in our earlier studies [26,39,40]. Electron microscope, dynamic light scattering (DLS), and Atomic Force Microscopy (AFM) analysis showed the integrity and size of Lemon-derived nanovesicles produced at laboratory scale (LNVs), ranging between 50–80 nm [27,40]. Furthermore, the proteomic analysis showed that 56.7 % of proteins in our dataset overlapped with those previously identified as exosome proteins in mammalian models. Besides focusing on LNVs, we have recently characterized industrial Lemon-derived nanovesicles (iLNVs) at dimensional, morphological, and metabolomic levels [40]

In the current study, to evaluate the ability of LNVs and iLNVS to interact with mammalian cells, nanovesicles were labeled with PKH26 (red signal) and incubated with THLE-2 cells.

The LNVs and iLNVs doses were chosen based on our previous studies on other cellular and animal models [27,40]. In one of our works [40] 2.5 and 5 μg/mL doses were tested in THP1 M0 cells; preliminary data from THLE2 cells suggested that the 2.5 μg/mL dose was sufficient to produce a biological response, making it the preferred choice for this current study.

After 2 h and 6 h of treatment with 10 μg/mL or 25 μg/mL LNVs, and with 2.5 μg/mL iLNVs, immunofluorescence protocol was executed, and THLE-2 cells were observed at confocal microscopy. Fig. 2 shows the time-dependent internalization of LNVs and iLNVs.

3.2. Antioxidant effects of Lemon-derived nanovesicles on THLE-2 exposed to menadione

3.2.1. The treatment with LNVs and iLNVs does not alter cell viability and reduces ROS levels

To assess whether LNVs and iLNVs affect hepatocyte cell viability, the MTT assay was performed.

The doses have been selected according to our previous studies using vesicles obtained through two distinct approaches [27,40]. As shown in Fig. 3A, 24 h of treatment with LNVs (10 μg/mL and 25 μg/mL) and iLNVs (2.5 μg/mL) does not induce a reduction in cell viability.

As mentioned above, different factors can induce ROS production in hepatocytes [5], potentially triggering liver disease. To explore the

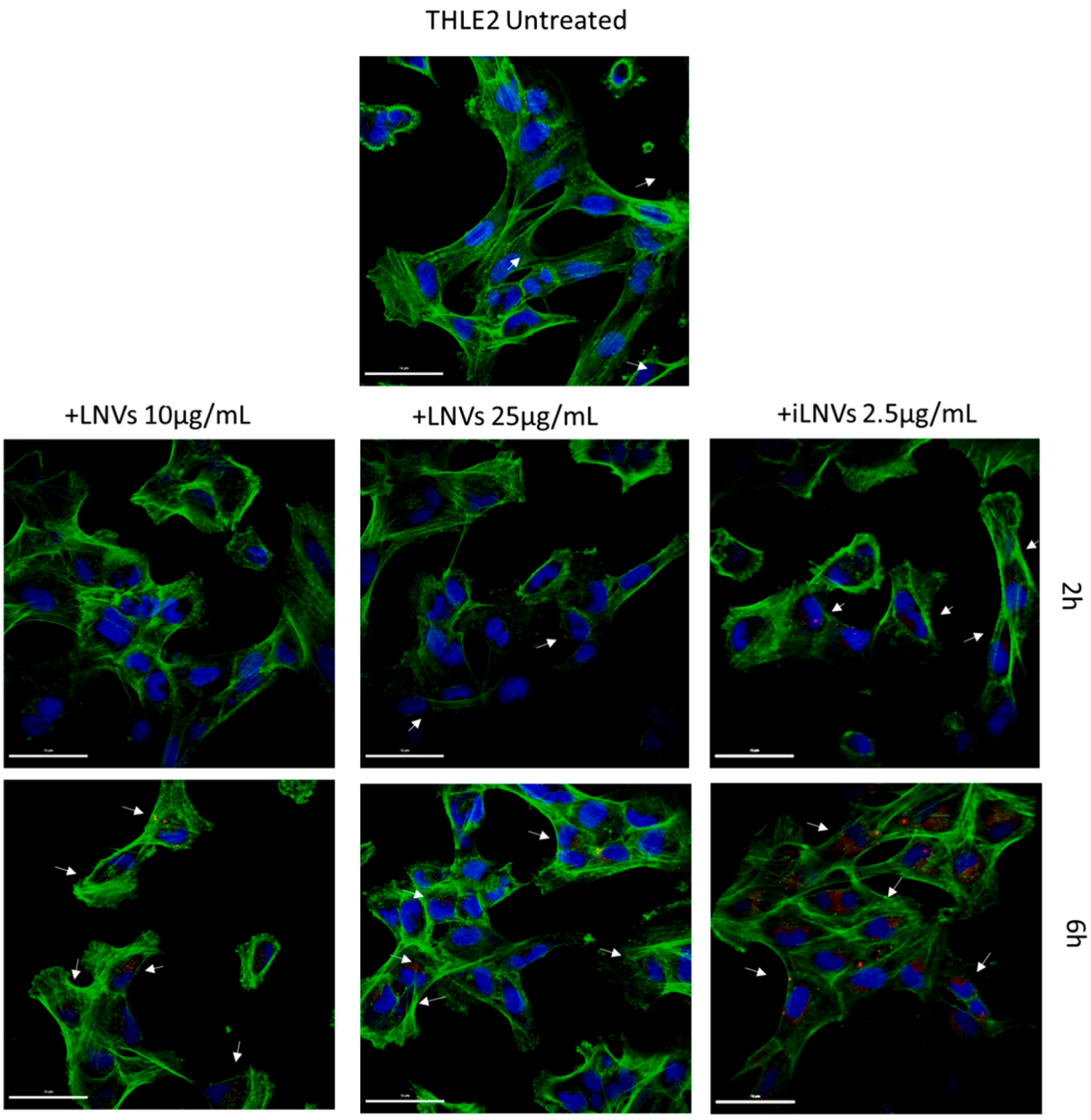

Fig. 2. : LNVs and iLNVs are internalized by THLE-2. Confocal microscopy images show the internalization of LNVs (10 µg/mL and 25 µg/mL) and iLNVs (2.5 µg/mL) by THLE-2 after 2 h and 6 h of treatment. LNVs and iLNVs were labeled red with PKH26, nuclei were stained blue with Hoechst, and cytoskeletons were stained green with Actin green.

possible antioxidant properties of LNVs and iLNVs in human healthy hepatocytes, ROS production was quantified after exposure to menadione, a well-known pro-oxidant molecule. Compared to untreated cells, menadione at both 5 and 10 µM doses induces an increase in ROS levels (Figure S1). As shown in Fig. 3B, we found a significant reduction of ROS levels in THLE-2 pre-treated for 24 hours with LNVs (10 and 25 µg/mL) or iLNVs (2.5 µg/mL) and subsequently subject for 30 and 60 minutes with menadione 5 µM (Fig. 3B, upper panel) and 10 µM (Fig. 3B, lower panel) compared to the cells treated with menadione alone. This effect is more evident in hepatocytes treated with the 5 µM dose of menadione compared to those treated with the 10 µM dose.

This data validates that the pre-treatment of both LNVs and iLNVs can exert an antioxidant effect in THLE-2 cells stimulated with menadione.

3.2.2. The pre-treatment with LNVs and iLNVs regulates Nrf2/HO-1 pathway in vitro

After confirming LNVs and iLNVs' ability to decrease ROS levels in THLE-2 cells, we investigated the signaling involved in the antioxidant response mediated by the nanovesicles. Specifically, we studied the Nrf2/HO-1 signaling pathway, since previous studies demonstrated its pivotal role in the antioxidant response [27] and its involvement in the LNV-mediated antioxidant mechanism [28]. The protein expression of Nrf2 (Fig. 4A and Figure S2) was evaluated in cells pre-treated for 24 hours with LNVs (10 µg/mL and 25 µg/mL) or iLNVs (2.5 µg/mL) and subsequently subjected to a 30-minute treatment with menadione (5 µM). When THLE-2 cells were pre-treated with LNVs or iLNVs, Nrf2 protein expression was upregulated compared to treatment with menadione alone; this upregulation is statistically significant in cells pre-treated with 10 and 25 µg/mL of LNVs.

Furthermore, as Nrf2 is a crucial antioxidant transcription factor

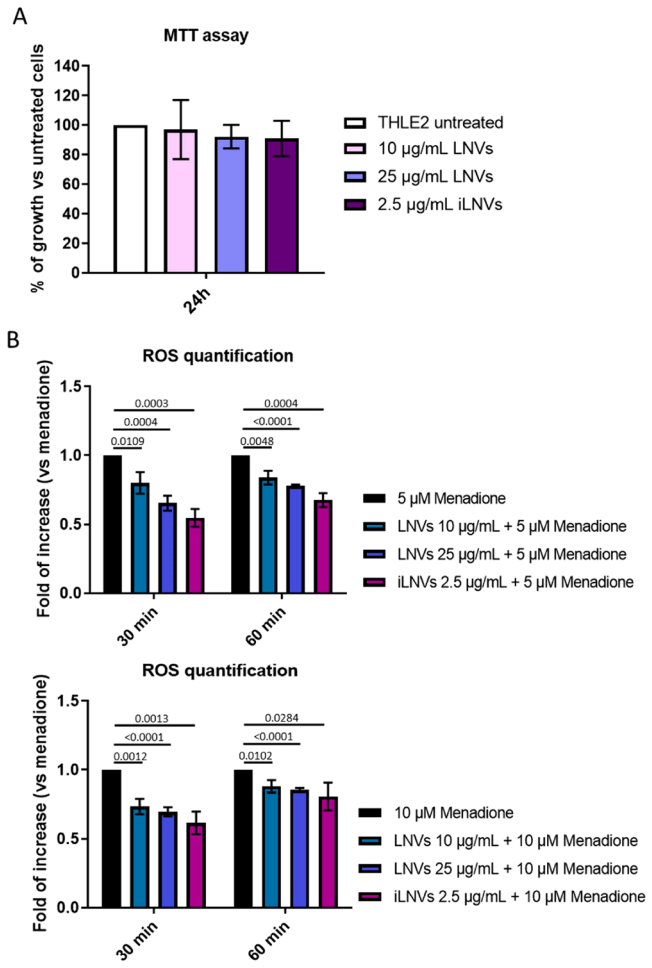

Fig. 3. The treatment with LNVs and iLNVs does not alter cell viability and reduces intracellular ROS production. A) THLE-2 cell viability was evaluated by MTT assay after 24 h of treatment with LNVs (10 µg/mL and 25 µg/mL) and iLNVs (25 µg/mL). Histograms show the percentage of cell viability compared to untreated cells (cn), with values presented as mean ± SD (n=3–4). B) THLE-2 cells were pre-treated with LNVs (10 µg/mL and 25 µg/mL) or iLNVs (2.5 µg/mL) for 24 hours, then exposed to 5 µM (upper panel) and 10 µM (lower panel) menadione for 30 and 60 minutes and to DCFDA. Fluorescence intensity indicate ROS levels. Values are shown as mean ± SD (n=3). Statistical significance between groups (menadione-treated cells vs. LNVs/iLNVs pre-treated + menadione) was determined using a two-tailed Student's t-test.

capable of translocating in the nucleus, we demonstrated its activation by examining both the total and nuclear fractions. In-depth, through confocal analysis, we observed a significant increase in the total and nuclear levels of Nrf2 (Fig. 4B) in LNVs/iLNVs pre-treated THLE-2, confirming the ability of nanovesicles to stimulate Nrf2 expression. This finding is pivotal since Nrf2 can determine the transcription of crucial antioxidant molecules such as HO-1. Consequently, we investigated the protein expression of HO-1 (Fig. 4C and Figure S3) and we observed a trend of increase in HO-1 protein expression after 24-hour pre-treatment with LNVs or iLNVs. These data support the correlation between LNVs/iLNVs antioxidant effects and these two mediators of the antioxidant response.

3.3. Effects of iLNV supplementation on body weight

In the *in vivo* model, the animals were initially balanced under basal conditions with comparable average weights at T0. In order to induce MetS, rats were fed with HFD for 10 weeks (from T0 to T1) and then (from T1 to T2) they were supplemented daily with iLNVs or vehicles. At the end of the experiment (T2), final body weight was statistically compared using a two-tailed Student's t-test, that outlined significant differences between HFD and HFD-iLNVs ($t = 2.359$; $df=8$; $p=0.046$; Fig. 5A). Also, body weight gains, calculated with respect to initial weight (T0), showed significant decreases in HFD-iLNVs versus HFD ($t = 4.119$; $df=8$; $p=0.003$; Fig. 5B).

3.4. Effects of iLNV supplementation on glucose tolerance and lipid homeostasis

The GTT performed at T2 outlined significant differences between HFD and HFD-iLNVs in glucose homeostasis, by evaluating the AUC. The student's t-test highlighted a decrease in HFD-iLNVs vs. HFD group ($t = 2.96$, $df = 8$, $p = 0.018$, Fig. 6A).

As for lipid homeostasis, plasma samples were collected from groups to observe eventual modifications in lipid profile in MetS following treatment with iLNVs at T2. Statistical analyses evidenced significant reductions of TG levels in HFD rats supplemented with iLNVs ($U=2$; $p=0.038$; Fig. 6B). The parameters related to cholesterol levels showed a non-significant variation of total cholesterol levels, a marked decrease in LDL cholesterol ($t = 4.874$, $df = 8$, $p = 0.0012$, Fig. 6C), and a related increase in HDL cholesterol ($t = 2.744$, $df = 8$, $p = 0.0253$, Fig. 6C) in HFD-iLNVs rats compared to HFD group.

3.5. Impact of iLNV supplementation on plasma redox homeostasis biomarkers

At T2, we assessed antioxidant and pro-oxidant status in both groups of rats. Notably, statistical significance emerged from the analysis of plasma samples related to the systemic pro-oxidant status. Indeed, iLNVs supplementation in HFD rats reduced both dROMs and LP-Cholox levels compared to the HFD group (respectively: $t = 3.73$, $df = 8$, $p = 0.0058$ and $t = 9.57$, $df = 8$, $p<0.0001$, as illustrated in Fig. 7A).

Furthermore, it was revealed a significant amelioration in the antioxidant capacity of animals in the HFD-iLNVs group compared to the HFD group. Specifically, an unpaired t-test was conducted on the values of the SHp and endogenous Anti-ROMs test, indicating a significant increase in HFD-iLNVs compared to HFD (respectively: $t = 3.22$, $df = 8$, $p = 0.012$ and $t = 2.864$, $df = 8$, $p = 0.021$, as shown in Fig. 5B). Non-significant differences were observed in the analysis of exogenous Anti-ROMs (Fig. 7B).

3.6. The administration of iLNVs regulates Nrf2/HO-1 signaling in HFD-fed rats liver

Also in the *in vivo* experiments, in accordance with the *in vitro* part of the study, Nrf2 and HO-1 modulation were investigated in the HFD rat's liver. In detail, we observed a significant increase of Nrf2 and HO-1 transcript levels in the HFD-iLNVs rat group compared to the untreated HFD-fed rats (Fig. 8A). Furthermore, the statistically significant upregulation of HO-1 was validated at the protein level, whereas for Nrf2, we observed a non-significant increasing trend in the HFD-iLNVs group (Fig. 8B and Figure S4). Nevertheless, immunohistochemical analysis of the hepatic tissue strongly indicated that Nrf2 is predominantly cytoplasmic in untreated HFD-fed rats, but it is mostly nuclear in the iLNV-treated group (Fig. 8C). As a result, the data reported herein confirm the activation of Nrf2/HO-1 antioxidant signaling in the livers of rats administrated with iLNVs.

4. Discussion

Citrus fruits are worldwide recognized to be essential elements in the everyday diet. Within Citrus limon, there are several essential natural compounds, including flavonoids, minerals, essential oils, and carotenoids, all known for their positive impact on health, due to their natural anti-inflammatory and antioxidant characteristics [43]. However, one of

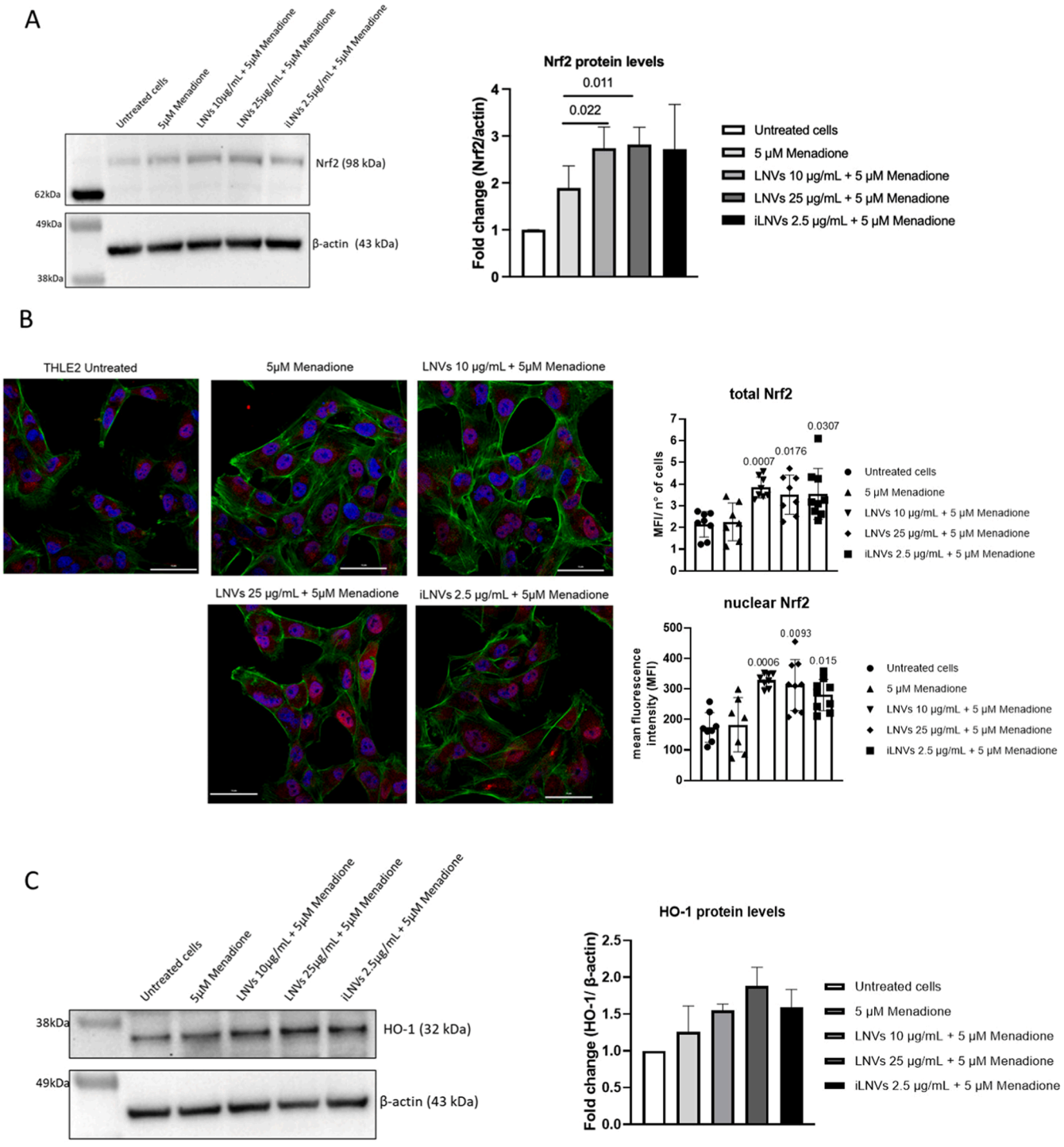

Fig. 4. The pre-treatment with LNVs and iLNVs regulates the Nrf2/HO-1 pathway *in vitro*. A) Western Blot analysis of Nrf2 and β-actin in THLE-2 pre-treated with LNVs/iLNVs for 24 h and with menadione (5 μM) for 30 minutes. B) Confocal microscopy of THLE-2 cells pre-treated with LNVs/iLNVs for 24 h and with menadione (5 μM) for 30 minutes. THLE-2 cells were stained for Nrf2 and labeled with Hoechst for nuclear visualization (blue) and with Actin Green for the cytoskeleton (green). The histograms show the quantification of the total (upper panel) and nuclear (lower panel) Nrf2; the data are the mean±SD (n=7–9). The statistical significance of the differences was analyzed using a two-tailed Student's t-test. C) Western Blot analysis of HO-1 and β-actin in THLE-2 pre-treated with LNVs/iLNVs for 24 h and with menadione (5 μM) for 30 minutes. Densitometric analysis values are the mean (± SD) of the normalized protein levels against the loading control (n=4).

the major problems with the dietary intake of natural compounds is their low stability and bioavailability caused by their reduced absorption and the digestive activity of the organism. From this premise arises the scientific community's interest in plant-derived nanovesicles, recognized for their distinctive characteristics, such as low immunological risk and, notably, heightened bioavailability. Their lipidic biolayer can exert an essential role in the preservation of the metabolites, RNA, and proteins packed into them, increasing the bioavailability of all these compounds [44–46].

Here, we aim to investigate the hepatoprotective effect of Lemon nanovesicles in THLE-2 cells and HFD-fed rat model. Findings correlated to plant-derived nanovesicles have indeed emerged as a crucial starting

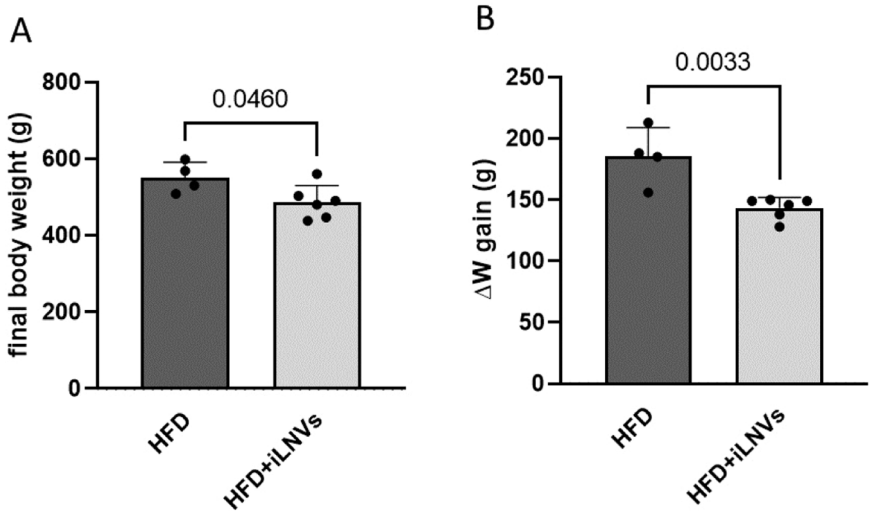

Fig. 5. iLNVs reduce body weight in HFD-fed rats. A-B) The final body weight and the weight gain T2-T0 were measured. The statistical differences between the two groups (iLNVs-HFD vs the HFD group) was analyzed using a two-tailed Student's t-test.

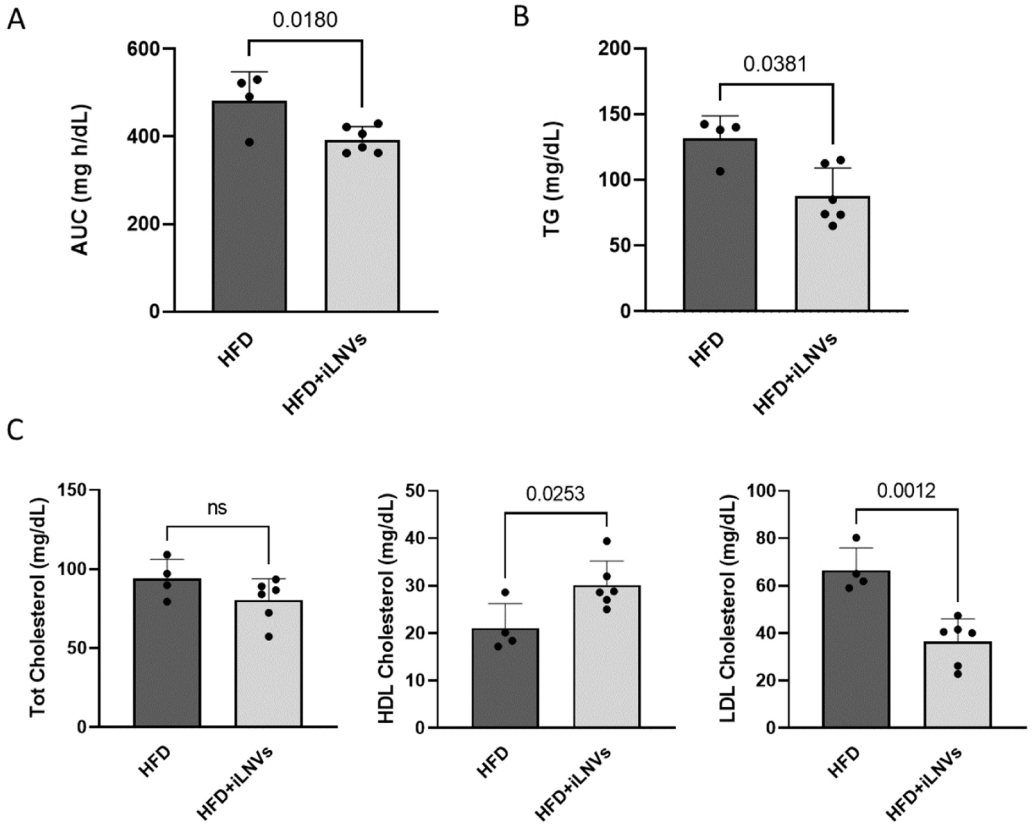

Fig. 6. iLNVs improve glucidic and lipid homeostasis altered in HFD-fed rats. HFD-fed rats were orally administered for 4 weeks with 1.2 mg/Kg of iLNVs and we measured A) AUC, B) TG, C) Total Cholesterol, LDL and HDL were measured with commercial kits. The statistical significance of the differences between the two groups (iLNVs-HFD vs the HFD group) was analyzed using a two-tailed Student's t-test.

point for investigating and understanding cross-kingdom communication and numerous studies have been conducted to analyze the interaction between nanovesicles derived from plants and mammalian targets.

Our study focuses not only on the evaluation of the hepatoprotective effects of nanovesicles produced in the laboratory but also on those produced on an industrial scale. Industrial production may represent a useful and excellent way to have easier access to lemon nanovesicles making them better applicable in the therapeutic and nutraceutical fields allowing a large-scale use. We have previously conducted a qualitative and quantitative metabolomic characterization of lemon nanovesicles produced at laboratory scale [39] and at industrial scale [40], showing overlapping profiles in terms of flavonoid and organic acid content.

Nowadays, antioxidants derived from plants are directly employed to tackle diseases linked to oxidative stress [47]. In their research, Savcı

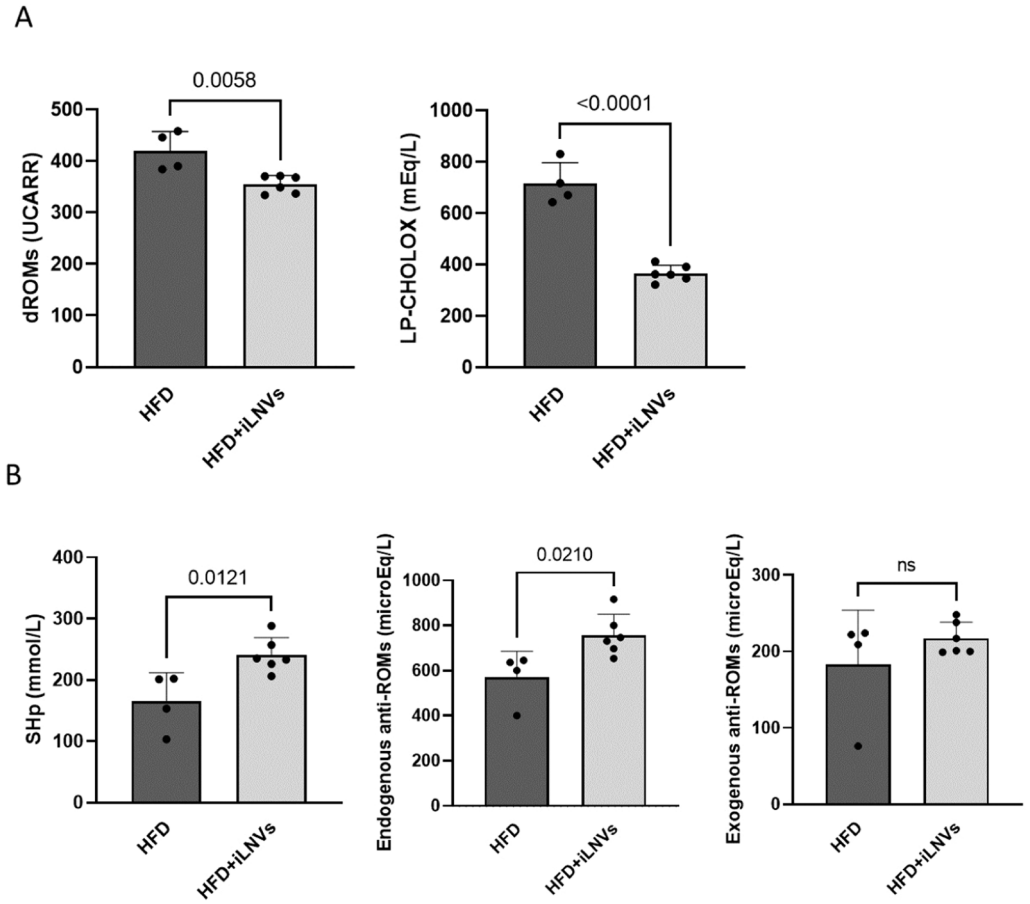

Fig. 7. iLNVs reduce systemic oxidative stress and increase systemic antioxidants. After the HFD-fed rats were orally administered for 4 weeks with iLNVs (1.2 mg/Kg), A) systemic oxidative stress parameters d-ROM and LP-CHOLOX and B) systemic antioxidants SHp, endogenous anti-ROMs (SH, uric acid, polyphenols) and exogenous anti-ROMs (vitamin C, vitamin E). The differences between the iLNVs-HFD and the HFD group were evaluated for statistical significance using a two-tailed Student's t-test.

et al. evaluated how EVs isolated from grapefruit promote wound healing [30] and reduce the level of intracellular ROS increased via H_2O_2-induced oxidative stress in HaCaT cells. In accordance with that, we recently found the capability of LNVs in reducing ROS levels and in activating the antioxidant pathway of Nrf2 in a fibroblast model stimulated with H_2O_2 and UVB, and in zebrafish embryos stimulated with LPS [27]. Here, we further expanded our data and underlined the ability of LNVs and iLNVs to reduce ROS levels in human healthy hepatocytes stimulated with menadione, a quinone and vitamin K analog. Menadione has the capability to transfer electrons from ETC complex I to oxygen, thereby producing superoxide [48], and has been widely used to induce oxidative stress and cell damage [49–52].

Undoubtedly, overproduction of ROS is a primary mechanism contributing to mitochondrial dysfunction, leading to lipid peroxidation and that consequently can induce the development of several diseases, such as hepatic disorders [53,54]. To maintain the level of ROS at a physiological level, the liver is equipped with various antioxidant systems with enzymatic activity. Among these processes, some rely on the activation of ARE, in turn regulated by Nrf2 [8] whose gene expression can be modulated by administering nanoparticles derived from plants [28].

For example, studies have shown that nanovesicles derived from Aloe vera contribute to wound healing by exerting antioxidant effects, by the activation of Nrf2 signaling [55]. In line with this, Ginger EVs, increased the nuclear translocation of Nrf2, which is implicated in the modulation of antioxidant-related gene, such as HO-1 [56]. In this study, we demonstrate that LNVs and iLNVs can induce the upregulation of the Nrf2/HO-1 signaling and a higher expression of nuclear Nrf2, which is consequently associated with its active transcriptional status.

Considering these powerful beneficial properties, plant-derived nanovesicles can be used to prevent or fight against multiple diseases. Recent studies indicate that exosome-like nanovesicles derived from yams may serve as effective oral treatments for osteoporosis [57], whereas nanovesicles from orange juice might be useful for managing obesity-related intestinal issues [58]. Furthermore, a recent study validates the therapeutic benefits of turmeric-derived nanoparticles (TDNPs), which contain natural bioactive compounds. TDNPs reduce oxidative stress, support fibroblast activity, and shift macrophage polarization, restoring the communication between fibroblasts and macrophages and accelerating diabetic wound healing [59]. In line with these studies, plant-derived nanovesicles can also exert hepatoprotective effects *in vivo*. Ginger-derived nanoparticles possess a protective impact against alcohol-induced liver damage in mice [56] while the administration of mice with blueberry-exosome-like nanovesicles improves liver function, halts vacuole formation, and reduces the accumulation of lipid droplets in the livers of animals exposed to a high-fat diet [28].

In addition to the evaluation of the effects of the nanovesicles on *in vitro* models, in our study, we reported the hepatoprotective effect of iLNVs in HFD-fed rats with MetS. NAFLD, the hepatic manifestation of MetS, is indeed one of the main causes of loss of hepatic function in the Western world and is often correlated with type 2 diabetes and obesity [60,61]. In obesity conditions, the gathering of fat in the abdominal area influences both lipid and glucose metabolism, resulting in a fat-laden and insulin-resistant liver [62]. Our results reveal that the oral

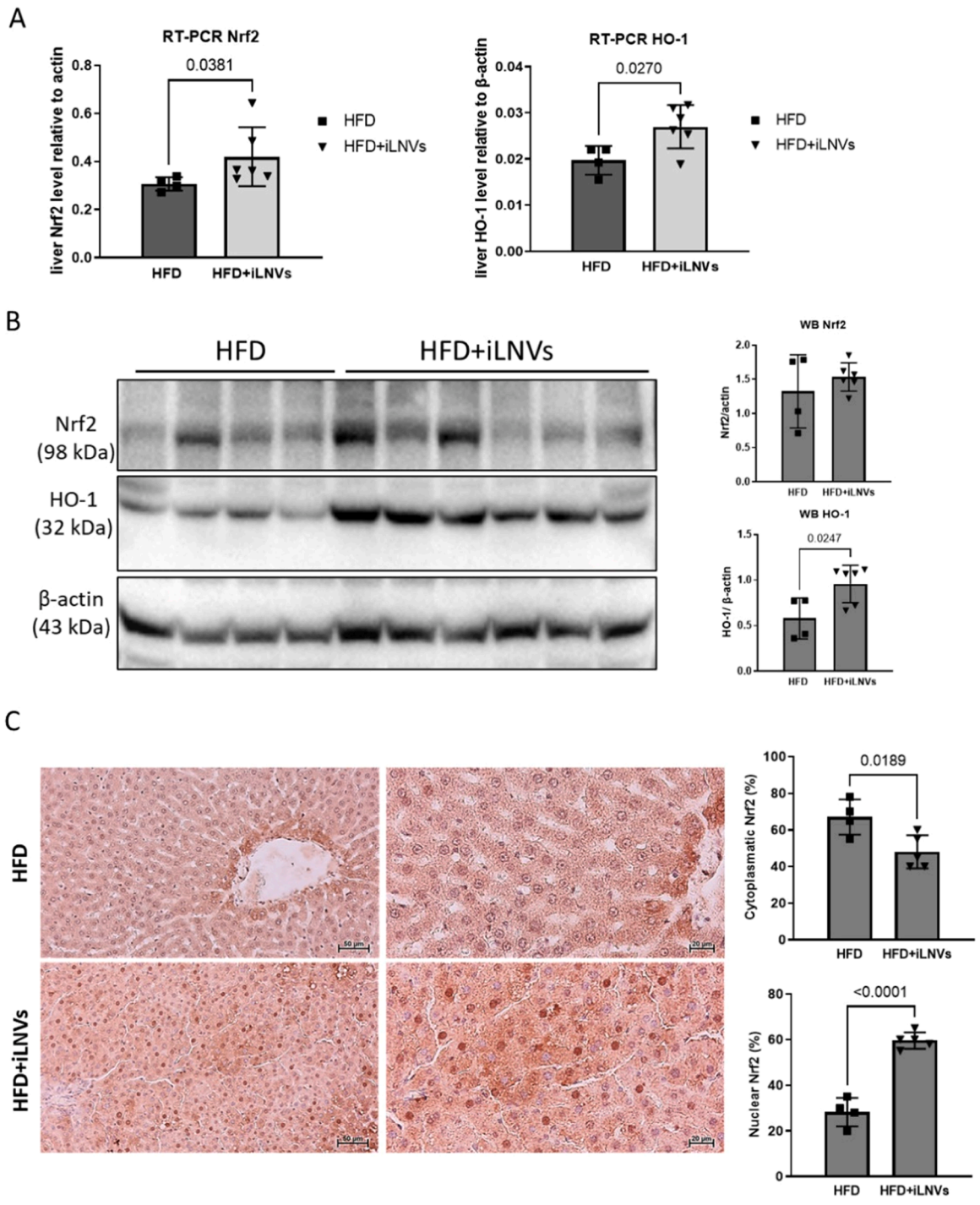

Fig. 8. iLNVs regulate Nrf2/HO-1 signaling in the liver of HFD-fed rats. A) qRT-PCR analysis assessed the ex vivo-mediated modulation of Nrf2 and HO-1 transcription levels by iLNVs in HFD rats. Results were expressed as Nrf2 and HO-1 levels normalized to the housekeeping gene, actin ($2^{\wedge} \Delta Ct$). Statistical significance between groups (HFD vs iLNVs-HFD) was determined using a two-tailed Student's t-test. B) Western Blot analysis of Nrf2, HO-1, and β-actin in hepatic tissues from iLNVs-HFD rats. Densitometric analysis values represent the mean (±SD) of normalized protein levels relative to the loading control. C) Immunohistochemical evaluation of Nrf2 in liver sections from both groups. Images were captured at 200x and 400x magnification, with scale bars of 50 μm and 20 μm, respectively. The percentage of immunopositivity was calculated based on high-power-field (HPF, magnification 400x) evaluations. Histograms depict the immunohistochemistry results, showing means ± SD of ten evaluations per group. Statistical differences between groups (iLNVs-HFD vs HFD) were analyzed using a two-tailed Student's t-test.

administration of iLNVs for 4 weeks to HFD rats is linked to an improvement in biometric parameters such as the final body weight and the body weight gained by rats throughout the study. These favorable outcomes are in line with the amelioration of glucose and lipid homeostasis encountered in HFD rats supplemented with iLNVs. Indeed, we demonstrated that iLNVs ameliorated glucose tolerance by reducing AUC. This supports the idea that administering natural compounds to HFD-fed animals can influence the deleterious effect of MetS on glucose metabolism by decreasing blood glucose levels, inducing a hypoglycemic effect, and improving the histopathological characteristics of

hepatic tissue [13,63]. Moreover, plant derivates can improve the homeostasis of lipid parameters in the HFD-fed state. Accordingly, here we found that iLNVs can decrease TG and LDL levels and can increase the amount of HDL cholesterol. The effects of iLNVs on lipid homeostasis, support their functional modulatory role, which is indicative of improved hepatic lipogenesis.

Crucially, our assessment of plasma redox balance unveiled that systemic oxidants are markedly reduced, alongside an enhancement of antioxidant defenses such as SHp and endogenous anti-ROMs.

In particular, the improved markers of oxidative state suggest that after iLNVs the hepatic production of primary lipoperoxide and hydroperoxide radicals, respectively assessed by LP-Cholox and dROMs, is reduced. Hydroperoxides, along with lipoperoxidation, have been identified as significant factors contributing to severe alterations that initiate oxidative damage in the liver of both humans and animals [64].

In accordance with this, we found improved levels of SHp and of the endogenous antiROMs also including the antioxidant defenses exerted by uric acid, bilirubin, and polyphenols. However, the non-significant effect of iLNVs on exogenous antiROMs, in terms of vitamins, agrees with the low levels of liposoluble vitamins present in the iLNVs [40]. In this context, SHp level is an established marker of endogenous antioxidant status since it denotes the homeostasis between thiols and disulfides, essential for cellular signaling pathways including, cell signaling cascades, apoptosis, detoxification processes, enzymatic efficacy, and transcriptional regulation [65]. Excessive production of reactive oxygen species (ROS) can lead to the oxidation of thiol groups, forming disulfide bridges and shifting the balance toward a more oxidized state. However, this process is reversible and treatments that enhance endogenous antioxidant defenses can shift the balance back in favor of thiols, as observed following iLNVs supplementation in our research and in previous studies[13,66]. Intriguingly, Nfr2 has been indicated as an upstream activator of the thiol-dependent redox signaling [67], hence supporting the putative influence of iLNVs on Nrf2/HO-1 antioxidant signaling which we found up-regulated in HFD rat liver. Nrf2 indeed regulates the expression of various thiol-based antioxidant enzymes, such as thioredoxin 1 and its corresponding reductase, sulfiredoxin, and peroxiredoxins 1 and 6 [68–70]. Consequently, the treatment with iLNVs could determine the activation of endogenous antioxidant mechanisms and have an effect in reducing Nrf2-mediated oxidation of thiol groups. In connection with this, we presumed that the antioxidant and hepatoprotective effect of lemon nanovesicles is not mediated by the action of a single compound, but by the combination of multiple contents within the nanovesicles and protected by the lipidic bilayer. Therefore, lemon-derived nanovesicles can be considered efficient vehicles, able to release their content inside mammalian cells. This is the main step to understand the recent intriguing aspect of the cross-kingdom interaction and its revolutionary and functional role in regulating mammalian pathological processes, such as hepatic disease.

Conclusions and limitations of the study

To conclude, lemon nanovesicles could be applied to human health, particularly for their role in disease prevention. Furthermore, here we demonstrated for the first time the antioxidant and hepatoprotective properties of nanovesicles isolated from lemon both *in vitro*, using human healthy hepatocytes, and *in vivo*, in HFD-fed rats. Despite the promising results obtained in demonstrating the antioxidant and hepatoprotective effects of lemon nanovesicles, further investigations will be necessary to determine the pathways responsible for nanovesicle effects. While in this study we focused on Nrf2/HO-1 signaling, additional molecular pathways can be investigated, for example, those mediated by RNA delivered by LNVs. Further studies will be also aimed at evaluating whether the effects of nanovesicles could be gender-related in the HFD rat model.

Inclusion and diversity

we support inclusive, diverse, and equitable conduct of research.

Resource Availability

Further information and requests for resources and reagents should be directed to and will be fulfilled by the corresponding author.

CRediT authorship contribution statement

Roberta Gasparro: Writing – original draft, Investigation. **Francesco Paolo Zummo:** Investigation. **Giuseppe Vergilio:** Investigation. **Giulia Duca:** Investigation. **Simona Fontana:** Writing – review & editing. **Giuditta Gambino:** Writing – original draft, Investigation, Data curation, Conceptualization. **Francesca Rappa:** Investigation, Data curation. **Nima Rabienezhad Ganji:** Investigation. **Monica Frinchi:** Investigation. **Nicolò Ricciardi:** Investigation. **Stefania Raimondo:** Writing – review & editing, Writing – original draft, Supervision, Project administration, Funding acquisition, Data curation, Conceptualization. **Valentina Di Liberto:** Writing – review & editing, Investigation, Funding acquisition. **Pierangelo Sardo:** Writing – review & editing. **Danila Di Majo:** Investigation. **Alice Conigliaro:** Writing – review & editing, Investigation. **Giulia Urone:** Investigation. **Riccardo Alessandro:** Writing – review & editing, Funding acquisition, Conceptualization. **Vincenza Tinnirello:** Investigation. **Giuseppe Ferraro:** Writing – review & editing.

Declaration of Competing Interest

The authors declare that there are no conflicts of interest that could be perceived as prejudicing the impartiality of the research reported. The authors S.R., A.C., and R.A. are cofounders of Navhetec, an Academic Spin-Off of the University of Palermo that only provides the nanovesicle extracts but that did not have any role in the conceptualization of this article and the analysis of the results. The same authors are inventors of the Italian patents 102019000005090 and 102015902344749.

Data availability

Data will be made available on request.

Acknowledgements

This work was fund by a grant from the University of Palermo (Incentivi ad attivita' di ricerca interdisciplinare, numero repertorio: 1105/2023; principal investigator Stefania Raimondo. Collaborators: Giuditta Gambino, Riccardo Alessandro, Giuseppe Ferraro) and in part by FFR 2023 from the University of Palermo to Valentina Di Liberto. R. G., G.D. and V.T. are PhD students in "Biomedicina, Neuroscienze e Diagnostica Avanzata" at the University of Palermo.

Appendix A. Supporting information

Supplementary data associated with this article can be found in the online version at doi:10.1016/j.biopha.2024.117532.

References

[1] H. Nohl, A.V. Kozlov, L. Gille, K. Staniek, Cell respiration and formation of reactive oxygen species: facts and artefacts, Biochem Soc. Trans. 31 (2003) 1308–1311, https://doi.org/10.1042/bst0311308.

[2] M. Herb, A. Gluschko, K. Wiegmann, A. Farid, A. Wolf, O. Utermohlen, O. Krut, M. Kronke, M. Schramm, Mitochondrial reactive oxygen species enable proinflammatory signaling through disulfide linkage of NEMO, Sci. Signal 12 (2019), https://doi.org/10.1126/scisignal.aar5926.

[3] A. Gluschko, M. Herb, K. Wiegmann, O. Krut, W.F. Neiss, O. Utermohlen, M. Kronke, M. Schramm, The beta(2) Integrin Mac-1 Induces Protective LC3-Associated Phagocytosis of Listeria monocytogenes, e325, Cell Host Microbe 23 (2018) 324–337, https://doi.org/10.1016/j.chom.2018.01.018.

[4] A.C. Bulua, A. Simon, R. Maddipati, M. Pelletier, H. Park, K.Y. Kim, M.N. Sack, D. L. Kastner, R.M. Siegel, Mitochondrial reactive oxygen species promote production of proinflammatory cytokines and are elevated in TNFR1-associated periodic syndrome (TRAPS), J. Exp. Med 208 (2011) 519–533, https://doi.org/10.1084/jem.20102049.

[5] P. Muriel, K.R. Gordillo, Role of Oxidative Stress in Liver Health and Disease, Oxid. Med Cell Longev. 2016 (2016) 9037051, https://doi.org/10.1155/2016/9037051.

[6] I.H. Kim, T. Kisseleva, D.A. Brenner, Aging and liver disease, Curr. Opin. Gastroenterol. 31 (2015) 184–191, https://doi.org/10.1097/MOG.0000000000000176.

[7] J. Zhou, Q. Zheng, Z. Chen, The Nrf2 Pathway in Liver Diseases, Front Cell Dev. Biol. 10 (2022) 826204, https://doi.org/10.3389/fcell.2022.826204.

[8] K. Itoh, N. Wakabayashi, Y. Katoh, T. Ishii, K. Igarashi, J.D. Engel, M. Yamamoto, Keap1 represses nuclear activation of antioxidant responsive elements by Nrf2 through binding to the amino-terminal Neh2 domain, Genes Dev. 13 (1999) 76–86, https://doi.org/10.1101/gad.13.1.76.

[9] X. Liu, Q. Zhu, M. Zhang, T. Yin, R. Xu, W. Xiao, J. Wu, B. Deng, X. Gao, W. Gong, G. Lu, Y. Ding, Isoliquiritigenin Ameliorates Acute Pancreatitis in Mice via Inhibition of Oxidative Stress and Modulation of the Nrf2/HO-1 Pathway, Oxid. Med Cell Longev. 2018 (2018) 7161592, https://doi.org/10.1155/2018/7161592.

[10] M.J. Alcaraz, M.L. Ferrandiz, Relevance of Nrf2 and heme oxygenase-1 in articular diseases, Free Radic. Biol. Med 157 (2020) 83–93, https://doi.org/10.1016/j.freeradbiomed.2019.12.007.

[11] E. Nanizawa, S. Otsuka, N. Hatayama, Y. Tamaki, Y. Hayashi, T. Ishikawa, S. Hirai, M. Naito, Short-term high-fat and high-carbohydrate diets increase susceptibility to liver injury by inducing hepatic procoagulant and proinflammatory conditions with different balances, Nutrition 101 (2022) 111710, https://doi.org/10.1016/j.nut.2022.111710.

[12] W.C. Huang, J.W. Xu, S. Li, X.E. Ng, Y.T. Tung, Effects of exercise on high-fat diet-induced non-alcoholic fatty liver disease and lipid metabolism in ApoE knockout mice, Nutr. Metab. (Lond.) 19 (2022) 10, https://doi.org/10.1186/s12986-022-00644-w.

[13] G. Gambino, G. Giglia, M. Allegra, V. Di Liberto, F.P. Zummo, F. Rappa, I. Restivo, F. Vetrano, F. Saiano, E. Palazzolo, G. Avellone, G. Ferraro, P. Sardo, D. Di Majo, Golden" Tomato Consumption Ameliorates Metabolic Syndrome: A Focus on the Redox Balance in the High-Fat-Diet-Fed Rat, Antioxid. (Basel) 12 (2023), https://doi.org/10.3390/antiox12051121.

[14] G. Gambino, M. Frinchi, G. Giglia, M. Scordino, G. Urone, G. Ferraro, G. Mudò, P. Sardo, D. Di Majo, V. Di Liberto, Impact of “Golden” tomato juice on cognitive alterations in metabolic syndrome: Insights into behavioural and biochemical changes in a high-fat diet rat model, J. Funct. Foods 112 (2024) 105964, https://doi.org/10.1016/j.jff.2023.105964.

[15] H. Manjunatha, K. Srinivasan, Hypolipidemic and antioxidant effects of curcumin and capsaicin in high-fat-fed rats, Can. J. Physiol. Pharm. 85 (2007) 588–596, https://doi.org/10.1139/y07-044.

[16] Y.J.W. Rozendaal, Y. Wang, Y. Paalvast, L.L. Tambyrajah, Z. Li, K. Willems van Dijk, P.C.N. Rensen, J.A. Kuivenhoven, A.K. Groen, P.A.J. Hilbers, N.A.W. van Riel, In vivo and in silico dynamics of the development of Metabolic Syndrome, PLoS Comput. Biol. 14 (2018) e1006145, https://doi.org/10.1371/journal.pcbi.1006145.

[17] D. Di Majo, P. Sardo, G. Giglia, V. Di Liberto, F.P. Zummo, M.G. Zizzo, G. F. Caldara, F. Rappa, G. Intili, R.M. van Dijk, D. Gallo, G. Ferraro, G. Gambino, Correlation of Metabolic Syndrome with Redox Homeostasis Biomarkers: Evidence from High-Fat Diet Model in Wistar Rats, Antioxid. (Basel) 12 (2022), https://doi.org/10.3390/antiox12010089.

[18] E. Rodriguez-Correa, I. Gonzalez-Perez, P.I. Clavel-Perez, Y. Contreras-Vargas, K. Carvajal, Biochemical and nutritional overview of diet-induced metabolic syndrome models in rats: what is the best choice? Nutr. Diabetes 10 (2020) 24, https://doi.org/10.1038/s41387-020-0127-4.

[19] G. Herrera, C.M. Silvero, M.C. Becerra, M. Lasaga, T. Scimonelli, Modulatory role of alpha-MSH in hippocampal-dependent memory impairment, synaptic plasticity changes, oxidative stress, and astrocyte reactivity induced by short-term high-fat diet intake, Neuropharmacology 239 (2023) 109688, https://doi.org/10.1016/j.neuropharm.2023.109688.

[20] V.H. Ortenzi, A.C. Oliveira, R.P. Vasconcelos, M.B. Neves, A.J. Teixeira, K. A. Oliveira, A.C.F. Ferreira, C.M. Takiya, R.S. Fortunato, High-fat diet elicits sex-based differences in liver inflammatory cytokines and redox homeostasis, Appl. Physiol. Nutr. Metab. (2024), https://doi.org/10.1139/apnm-2023-0457.

[21] J. Beltowski, G. Wojcicka, D. Gorny, A. Marciniak, The effect of dietary-induced obesity on lipid peroxidation, antioxidant enzymes and total plasma antioxidant capacity, J. Physiol. Pharm. 51 (2000) 883–896.

[22] A.A. Elmarakby, J.D. Imig, Obesity is the major contributor to vascular dysfunction and inflammation in high-fat diet hypertensive rats, Clin. Sci. (Lond.) 118 (2010) 291–301, https://doi.org/10.1042/CS20090395.

[23] S. Lasker, M.M. Rahman, F. Parvez, M. Zamila, P. Miah, K. Nahar, F. Kabir, S. B. Sharmin, N. Subhan, G.U. Ahsan, M.A. Alam, High-fat diet-induced metabolic syndrome and oxidative stress in obese rats are ameliorated by yogurt supplementation, Sci. Rep. 9 (2019) 20026, https://doi.org/10.1038/s41598-019-56538-0.

[24] A.P. Delli Bovi, F. Marciano, C. Mandato, M.A. Siano, M. Savoia, P. Vajro, Oxidative Stress in Non-alcoholic Fatty Liver Disease. An Updated Mini Review, Front Med (Lausanne) 8 (2021) 595371, https://doi.org/10.3389/fmed.2021.595371.

[25] S.K. Asrani, H. Devarbhavi, J. Eaton, P.S. Kamath, Burden of liver diseases in the world, J. Hepatol. 70 (2019) 151–171, https://doi.org/10.1016/j.jhep.2018.09.014.

[26] S. Raimondo, F. Naselli, S. Fontana, F. Monteleone, A. Lo Dico, L. Saieva, G. Zito, A. Flugy, M. Manno, M.A. Di Bella, G. De Leo, R. Alessandro, Citrus limon-derived nanovesicles inhibit cancer cell proliferation and suppress CML xenograft growth by inducing TRAIL-mediated cell death, Oncotarget 6 (2015) 19514–19527, https://doi.org/10.18632/oncotarget.4004.

[27] O. Urzi, M. Cafora, N.R. Ganji, V. Tinnirello, R. Gasparro, S. Raccosta, M. Manno, A.M. Corsale, A. Conigliaro, A. Pistocchi, S. Raimondo, R. Alessandro, Lemon-derived nanovesicles achieve antioxidant and anti-inflammatory effects activating the AhR/Nrf2 signaling pathway, iScience 26 (2023) 107041, https://doi.org/10.1016/j.isci.2023.107041.

[28] W.J. Zhao, Y.P. Bian, Q.H. Wang, F. Yin, L. Yin, Y.L. Zhang, J.H. Liu, Blueberry-derived exosomes-like nanoparticles ameliorate nonalcoholic fatty liver disease by attenuating mitochondrial oxidative stress, Acta Pharm. Sin. 43 (2022) 645–658, https://doi.org/10.1038/s41401-021-00681-w.

[29] B.H. Lee, S.C. Wu, H.Y. Chien, T.L. Shen, W.H. Hsu, Tomato-fruit-derived extracellular vesicles inhibit Fusobacterium nucleatum via lipid-mediated mechanism, Food Funct. 14 (2023) 8942–8950, https://doi.org/10.1039/d3fo01608k.

[30] Y. Savci, O.K. Kirbas, B.T. Bozkurt, E.A. Abdik, P.N. Tasli, F. Sahin, H. Abdik, Grapefruit-derived extracellular vesicles as a promising cell-free therapeutic tool for wound healing, Food Funct. 12 (2021) 5144–5156, https://doi.org/10.1039/d0fo02953j.

[31] J. Liu, W. Li, Y. Bian, X. Jiang, F. Zhu, F. Yin, L. Yin, X. Song, H. Guo, Garlic-derived exosomes regulate PFKFB3 expression to relieve liver dysfunction in high-fat diet-fed mice via macrophage-hepatocyte crosstalk, Phytomedicine 112 (2023) 154679, https://doi.org/10.1016/j.phymed.2023.154679.

[32] N.J. Liu, N. Wang, J.J. Bao, H.X. Zhu, L.J. Wang, X.Y. Chen, Lipidomic Analysis Reveals the Importance of GIPCs in Arabidopsis Leaf Extracellular Vesicles, Mol. Plant 13 (2020) 1523–1532, https://doi.org/10.1016/j.molp.2020.07.016.

[33] J. Xiao, S. Feng, X. Wang, K. Long, Y. Luo, Y. Wang, J. Ma, Q. Tang, L. Jin, X. Li, M. Li, Identification of exosome-like nanoparticle-derived microRNAs from 11 edible fruits and vegetables, PeerJ 6 (2018) e5186, https://doi.org/10.7717/peerj.5186.

[34] Z. Deng, Y. Rong, Y. Teng, J. Mu, X. Zhuang, M. Tseng, A. Samykutty, L. Zhang, J. Yan, D. Miller, J. Suttles, H.G. Zhang, Broccoli-Derived Nanoparticle Inhibits Mouse Colitis by Activating Dendritic Cell AMP-Activated Protein Kinase, Mol. Ther. 25 (2017) 1641–1654, https://doi.org/10.1016/j.ymthe.2017.01.025.

[35] T. Feng, W. Ahmed, T. Ahmed, L. Chen, Nanoparticles derived from herbal preparations May represent a novel nucleic acid therapy, e 20230029, Interdiscip. Med. 2 (2024), https://doi.org/10.1002/INMD.20230029.

[36] J. Mu, X. Zhuang, Q. Wang, H. Jiang, Z.B. Deng, B. Wang, L. Zhang, S. Kakar, Y. Jun, D. Miller, H.G. Zhang, Interspecies communication between plant and mouse gut host cells through edible plant derived exosome-like nanoparticles, Mol. Nutr. Food Res 58 (2014) 1561–1573, https://doi.org/10.1002/mnfr.201300729.

[37] D.K. Kim, W.J. Rhee, Antioxidative Effects of Carrot-Derived Nanovesicles in Cardiomyoblast and Neuroblastoma Cells, Pharmaceutics 13 (2021), https://doi.org/10.3390/pharmaceutics13081203.

[38] X. Zhao, F. Yin, L. Fu, Y. Ma, L. Ye, Y. Huang, W. Fan, W. Gao, Y. Cai, X. Mou, Garlic-derived exosome-like nanovesicles as a hepatoprotective agent alleviating acute liver failure by inhibiting CCR2/CCR5 signaling and inflammation, Biomater. Adv. 154 (2023) 213592, https://doi.org/10.1016/j.bioadv.2023.213592.

[39] S. Raimondo, O. Urzi, S. Meraviglia, M. Di Simone, A.M. Corsale, N. Rabienezhad Ganji, A. Palumbo Piccionello, G. Polito, E. Lo Presti, F. Dieli, A. Conigliaro, R. Alessandro, Anti-inflammatory properties of lemon-derived extracellular vesicles are achieved through the inhibition of ERK/NF-kappaB signalling pathways, J. Cell Mol. Med 26 (2022) 4195–4209, https://doi.org/10.1111/jcmm.17404.

[40] V. Tinnirello, M.G. Zizzo, A. Conigliaro, M. Tabone, N.R. Ganji, A. Cicio, C. Bressa, M. Larrosa, F. Rappa, G. Vergilio, R. Gasparro, A. Gallo, R.M. Serio, R. Alessandro, S. Raimondo, Industrial-produced lemon nanovesicles ameliorate experimental colitis-associated damages in rats via the activation of anti-inflammatory and antioxidant responses and microbiota modification, Biomed. Pharm. 174 (2024) 116514, https://doi.org/10.1016/j.biopha.2024.116514.

[41] S. Lee, J. Hashimoto, T. Suzuki, A. Satoh, The effects of exercise load during development on oxidative stress levels and antioxidant potential in adulthood, Free Radic. Res 51 (2017) 179–186, https://doi.org/10.1080/10715762.2017.1291939.

[42] G. Meineri, M. Giacobini, G. Forneris, Evaluation of physiological parameters of the plasma oxidative status in rabbits, J. Appl. Anim. Res. 45 (2017) 315–319, https://doi.org/10.1080/09712119.2016.1190734.

[43] Y. Wang, X.J. Liu, J.B. Chen, J.P. Cao, X. Li, C.D. Sun, Citrus flavonoids and their antioxidant evaluation, Crit. Rev. Food Sci. Nutr. 62 (2022) 3833–3854, https://doi.org/10.1080/10408398.2020.1870035.

[44] L. Chen, H. Cao, Q. Huang, J. Xiao, H. Teng, Absorption, metabolism and bioavailability of flavonoids: a review, Crit. Rev. Food Sci. Nutr. 62 (2022) 7730–7742, https://doi.org/10.1080/10408398.2021.1917508.

[45] M. Pinedo, L. de la Canal, C. de Marcos Lousa, A call for Rigor and standardization in plant extracellular vesicle research, J. Extra Vesicles 10 (2021) e12048, https://doi.org/10.1002/jev2.12048.

[46] J. Feng, Q. Xiu, Y. Huang, Z. Troyer, B. Li, L. Zheng, Plant-Derived Vesicle-Like Nanoparticles as Promising Biotherapeutic Tools: Present and Future, Adv. Mater. 35 (2023) e2207826, https://doi.org/10.1002/adma.202207826.
[47] M. Kumar, V. Pratap, A. Nigam, B. Sinha, M. Singh, J. Gour, Plants as a Source of Potential Antioxidants and Their Effective Nanoformulations, J. Sci. Res. 65 (2021) 57–72, https://doi.org/10.37398/jsr.2021.650308.
[48] B. Frei, K.H. Winterhalter, C. Richter, Menadione- (2-methyl-1,4-naphthoquinone-) dependent enzymatic redox cycling and calcium release by mitochondria, Biochemistry 25 (1986) 4438–4443, https://doi.org/10.1021/bi00363a040.
[49] M. Comporti, Three models of free radical-induced cell injury, Chem. Biol. Inter. 72 (1989) 1–56, https://doi.org/10.1016/0009-2797(89)90016-1.
[50] A. Halilovic, T. Schmedt, A.S. Benischke, C. Hamill, Y. Chen, J.H. Santos, U. V. Jurkunas, Menadione-Induced DNA Damage Leads to Mitochondrial Dysfunction and Fragmentation During Rosette Formation in Fuchs Endothelial Corneal Dystrophy, Antioxid. Redox Signal 24 (2016) 1072–1083, https://doi.org/10.1089/ars.2015.6532.
[51] G. Loor, J. Kondapalli, J.M. Schriewer, N.S. Chandel, T.L. Vanden Hoek, P. T. Schumacker, Menadione triggers cell death through ROS-dependent mechanisms involving PARP activation without requiring apoptosis, Free Radic. Biol. Med 49 (2010) 1925–1936, https://doi.org/10.1016/j.freeradbiomed.2010.09.021.
[52] W.F. Tzeng, J.L. Lee, T.J. Chiou, The role of lipid peroxidation in menadione-mediated toxicity in cardiomyocytes, J. Mol. Cell Cardiol. 27 (1995) 1999–2008, https://doi.org/10.1016/0022-2828(95)90021-7.
[53] A. Mansouri, C.H. Gattolliat, T. Asselah, Mitochondrial Dysfunction and Signaling in Chronic Liver Diseases, Gastroenterology 155 (2018) 629–647, https://doi.org/10.1053/j.gastro.2018.06.083.
[54] G.H. Koek, P.R. Liedorp, A. Bast, The role of oxidative stress in non-alcoholic steatohepatitis, Clin. Chim. Acta 412 (2011) 1297–1305, https://doi.org/10.1016/j.cca.2011.04.013.
[55] M.K. Kim, Y.C. Choi, S.H. Cho, J.S. Choi, Y.W. Cho, The Antioxidant Effect of Small Extracellular Vesicles Derived from Aloe vera Peels for Wound Healing, Tissue Eng. Regen. Med 18 (2021) 561–571, https://doi.org/10.1007/s13770-021-00367-8.
[56] X. Zhuang, Z.B. Deng, J. Mu, L. Zhang, J. Yan, D. Miller, W. Feng, C.J. McClain, H. G. Zhang, Ginger-derived nanoparticles protect against alcohol-induced liver damage, J. Extra Vesicles 4 (2015) 28713, https://doi.org/10.3402/jev.v4.28713.
[57] J.H. Hwang, Y.S. Park, H.S. Kim, D.H. Kim, S.H. Lee, C.H. Lee, J.E. Kim, S. Lee, H. M. Kim, H.W. Kim, J. Kim, W. Seo, H.J. Kwon, B.J. Song, D.K. Kim, M.C. Baek, Y. E. Cho, Yam-derived exosome-like nanovesicles stimulate osteoblast formation and prevent osteoporosis in mice, J. Control Release 355 (2023) 184–198, https://doi.org/10.1016/j.jconrel.2023.01.071.
[58] E. Berger, P. Colosetti, A. Jalabert, E. Meugnier, O.P.B. Wiklander, J. Jouhet, E. Errazurig-Cerda, S. Chanon, D. Gupta, G.J.P. Rautureau, A. Geloen, S. El-Andaloussi, B. Panthu, J. Rieusset, S. Rome, Use of Nanovesicles from Orange Juice to Reverse Diet-Induced Gut Modifications in Diet-Induced Obese Mice, Mol. Ther. Methods Clin. Dev. 18 (2020) 880–892, https://doi.org/10.1016/j.omtm.2020.08.009.
[59] B. Wu, W. Pan, S. Luo, X. Luo, Y. Zhao, Q. Xiu, M. Zhong, Z. Wang, T. Liao, N. Li, C. Liu, C. Nie, G. Yi, S. Lin, M. Zou, B. Li, L. Zheng, Turmeric-Derived Nanoparticles Functionalized Aerogel Regulates Multicellular Networks to Promote Diabetic Wound Healing, Adv. Sci. (Weinh.) 11 (2024) e2307630, https://doi.org/10.1002/advs.202307630.
[60] Z.M. Younossi, A.B. Koenig, D. Abdelatif, Y. Fazel, L. Henry, M. Wymer, Global epidemiology of nonalcoholic fatty liver disease-Meta-analytic assessment of prevalence, incidence, and outcomes, Hepatology 64 (2016) 73–84, https://doi.org/10.1002/hep.28431.
[61] C. Hobeika, M. Ronot, A. Beaufrere, V. Paradis, O. Soubrane, F. Cauchy, Metabolic syndrome and hepatic surgery, J. Visc. Surg. 157 (2020) 231–238, https://doi.org/10.1016/j.jviscsurg.2019.11.004.
[62] S. Stojsavljevic, M. Gomercic Palcic, L. Virovic Jukic, L. Smircic Duvnjak, M. Duvnjak, Adipokines and proinflammatory cytokines, the key mediators in the pathogenesis of nonalcoholic fatty liver disease, World J. Gastroenterol. 20 (2014) 18070–18091, https://doi.org/10.3748/wjg.v20.i48.18070.
[63] A. Hussain, J.S. Cho, J.S. Kim, Y.I. Lee, Protective Effects of Polyphenol Enriched Complex Plants Extract on Metabolic Dysfunctions Associated with Obesity and Related Nonalcoholic Fatty Liver Diseases in High Fat Diet-Induced C57BL/6 Mice, Molecules 26 (2021), https://doi.org/10.3390/molecules26020302.
[64] M. Rojkind, J.A. Dominguez-Rosales, N. Nieto, P. Greenwel, Role of hydrogen peroxide and oxidative stress in healing responses, Cell Mol. Life Sci. 59 (2002) 1872–1891, https://doi.org/10.1007/pl00012511.
[65] S. Biswas, A.S. Chida, I. Rahman, Redox modifications of protein-thiols: emerging roles in cell signaling, Biochem Pharm. 71 (2006) 551–564, https://doi.org/10.1016/j.bcp.2005.10.044.
[66] L. Turell, R. Radi, B. Alvarez, The thiol pool in human plasma: the central contribution of albumin to redox processes, Free Radic. Biol. Med 65 (2013) 244–253, https://doi.org/10.1016/j.freeradbiomed.2013.05.050.
[67] D. Dong, Y. Zhang, H. He, Y. Zhu, H. Ou, Alpinetin inhibits macrophage infiltration and atherosclerosis by improving the thiol redox state: Requirement of GSk3beta/Fyn-dependent Nrf2 activation, Faseb J 36 (2022) e22261, https://doi.org/10.1096/fj.202101567R.
[68] Y. Hirotsu, F. Katsuoka, R. Funayama, T. Nagashima, Y. Nishida, K. Nakayama, J. D. Engel, M. Yamamoto, Nrf2-MafG heterodimers contribute globally to antioxidant and metabolic networks, Nucleic Acids Res 40 (2012) 10228–10239, https://doi.org/10.1093/nar/gks827.
[69] B.N. Chorley, M.R. Campbell, X. Wang, M. Karaca, D. Sambandan, F. Bangura, P. Xue, J. Pi, S.R. Kleeberger, D.A. Bell, Identification of novel NRF2-regulated genes by ChIP-Seq: influence on retinoid X receptor alpha, Nucleic Acids Res 40 (2012) 7416–7429, https://doi.org/10.1093/nar/gks409.
[70] M. Dodson, A. Shakya, A. Anandhan, J. Chen, J.G.N. Garcia, D.D. Zhang, NRF2 and diabetes: the good, the bad, and the complex, Diabetes 71 (2022) 2463–2476, https://doi.org/10.2337/db22-0623.